EUROPEAN FUSION DEVELOPMENT AGREEMENT

EFDA–JET–CP(03)01-41

M.J. Mantsinen, L.-G. Eriksson, E. Gauthier, G.T. Hoang, E. Joffrin, R. Koch,
X.Litaudon, A. Lyssoivan, P. Mantica, M.F.F. Nave, J.-M. Noterdaeme,
C.C. Petty, O. Sauter, S.E. Sharapov and JET EFDA Contributors

Application of ICRF Waves in Tokamaks Beyond Heating

Application of ICRF Waves in Tokamaks Beyond Heating

M.J. Mantsinen[1], L.-G. Eriksson[2], E. Gauthier[2], G.T. Hoang[2], E. Joffrin[2], R. Koch[3],
X. Litaudon[2], A. Lyssoivan[3], P. Mantica[4], M.F.F. Nave[5], J.-M. Noterdaeme[6, 7],
C.C. Petty[8], O. Sauter[9], S.E. Sharapov[10] and JET EFDA Contributors*

[1]Helsinki University of Technology, Association Euratom-Tekes, Finland
[2]Association EURATOM/CEA, CEA Cadarache, Saint-Paul-Lez-Durance, France
[3]LPP-ERM/KMS, Association EURATOM-Belgian State, TEC, Brussels, Belgium
[4]Intituto di Fisica del Plasma, EURATOM-ENEA-CNR Association, Milan, Italy
[5]Associação EURATOM-IST, Centro de Fusão Nuclear, Lisboa, Portugal
[6]Max-Planck IPP-EURATOM Assoziation, Garching, Germany
[7]Gent University, EESA Department, Gent, Belgium
[8]General Atomics, San Diego, California, USA
[9]CRPP, Association EURATOM-Confédération Suisse, EPFL, Lausanne, Switzerland
[10]EURATOM/UKAEA Fusion Association, Culham Science Centre, Abingdon, Oxon., OX14 3DB, UK
**See Annex of J. Pamela et al., "Overview of Recent JET Results and Future Perspectives", Fusion Energy 2000 (Proc. 18th Int. Conf. Sorrento, 2000), IAEA, Vienna (2001).*

Preprint of Paper to be submitted for publication in Proceedings of the
EPS Conference on Controlled Fusion and Plasma Physics,
(St. Petersburg, Russia, 7-11 July 2003)

ABSTRACT
Interaction of waves in the Ion Cyclotron Range of Frequencies (ICRF) with a plasma has a number of key properties that make them attractive beyond pure heating. Firstly, the waves can interact resonantly with either the plasma ions or electrons. In the case of ion cyclotron damping, a small number of resonant ions are often accelerated to high energies. These ions, apart from heating the bulk plasma via Coulomb collisions, can increase fusion reactivity, affect plasma stability and drive current. They have also been invaluable in diagnostic applications and simulations of fusion-born 3.5MeV alpha particles. The second key property of ICRF waves is the transfer of wave momentum to the plasma. This allows one to drive current, affect plasma rotation and induce radial transport of the fast ions with toroidally directed waves. Finally, ICRF power deposition is rather narrow and its location can be externally controlled, which has important applications in improving the plasma performance, affecting the local plasma transport and providing a tool for plasma transport studies. Representative examples from present-day tokamak experiments are reviewed to highlight the available capabilities.

1. INTRODUCTION
Heating with fast magnetosonic waves in the Ion Cyclotron Range of Frequencies (ICRF) is a well-established method on present-day tokamaks and is envisaged as one of the main auxiliary heating techniques for ITER. Present-day experiments show that the application of ICRF waves has capabilities beyond pure heating which are directly applicable to ITER.

The potential of ICRF waves beyond heating results from the fundamental properties of ICRF waves and their interactions with the plasma particles. First, let us consider the resonant interaction of ICRF waves with ions, which takes place when $\omega = n\omega_{ci} + k_{||}v_{||}$, i.e. when the wave frequency matches the Doppler-shifted ion cyclotron frequency or its harmonic. When this interaction takes place, the wave energy is normally most effectively absorbed by either minority ions ($n = 1$) or ions with large Larmor-orbits ($n > 1$). Since the number of such ions is relatively small, power per particle is typically rather large. Consequently, the ions can attain high energies. Indeed, ions with energies up to the MeV-range are often measured during high power ICRF heating on existing tokamaks that are large enough to confine ions with such high energies. In addition to heating plasma via Coulomb collisions, the fast ions have been used to enhance fusion reactivity, affect plasma stability as well as to provide a source for plasma diagnostic applications and for simulations of fusion-born alpha particles and their effects on the plasma.

In the case of strong ion cyclotron damping, the ICRF power deposition is rather localised around $\omega \approx n\omega_{ci}$. Furthermore, since $\omega_{ci} = \omega_{ci}(R)$, the location of the power deposition can be externally controlled in the tokamak major radius R with the choice of ω The narrow and controllable ICRF power deposition has been important in improving the plasma performance e.g. in plasmas with internal transport barriers. The ICRF power deposition becomes particularly narrow when the fast waves are mode converted to short wavelength waves such as ion Bernstein waves, ion cyclotron waves or kinetic Alfven waves. Since it provides rather localised direct electron heating with prompt response to changes in the power waveform, ICRF mode conversion using power modulation techniques provides a suitable tool for electron heat transport investigations. Direct electron heating with the launched fast waves is also possible.

Further applications of ICRF waves arise from the momentum they carry. As the waves are absorbed, the wave momentum is also transferred to the plasma. This transfer of wave momentum to the plasma can be used to drive current. More recently, it has been used to influence plasma rotation and control the profile of resonating fast ions and thereby many ICRF-related quantities during ICRF heating. These effects are especially important in the case of toroidally directed waves. With toroidally symmetric waves, the momentum imparted by ICRF waves to the plasma is very small. This, together with the other properties of ICRF waves, make them attractive for simulating alpha-particle heating in ITER burning plasma scenarios. In particular, high-power ion cyclotron resonance heating with toroidally symmetric ICRF waves has been used for this purpose since it is similar in its characteristics to alpha-particle heating (bulk electron heating via high-energy ICRF-accelerated ions without applying net torque and fuelling).

Finally, the applicability of ICRF waves for low-V_{loop} plasma start-up assist and wall conditioning in the presence of magnetic field has been successfully demonstrated on present-day tokamaks. The paper is organised as follows. In Section 2 applications using ICRF-accelerated fast ions are discussed. This is followed by a discussion on current drive with ICRF waves in Sec.3. A number of recent experiments where the narrow ICRF power deposition profiles play a key role are presented in Section 4 and the effects of ICRF waves on plasma rotation are reviewed in Section 5. The application of toroidally symmetric ICRF waves to simulate heating by fusion-born alpha particles in ITER is the topic of Sect.6. The use of ICRF waves for wall conditioning and start-up assist is discussed in Sect.7. The conclusions are presented in Section 8.

2. APPLICATIONS OF FAST IONS ACCELERATED BY ICRF WAVES

Ion cyclotron damping at $\omega \approx n\omega_{ci}$ often accelerates the resonating ions to high energies. In this section, a number of experiments are discussed where ICRF-accelerated fast ions play a key role.

2.1 EFFECT OF ICRF-ACCELERATED IONS ON SAWTOOTH INSTABILITY

The first observations of the influence of ICRF-accelerated fast ions on plasma instabilities came with the dramatic increase in the coupled ICRF power in the tokamak experiments in 1980's. In particular, in experiments with central ICRH, stabilisation of sawtooth oscillations caused by the n=1/m=1 internal kink mode was observed [3, 4]. Here, m and n are the poloidal and toroidal mode numbers, respectively. The stabilising effect was found to be due to ICRF-heated ions having bounce-averaged precessional drift frequencies $\omega_{D,fast}$ in excess of the mode frequency [5].

Later on, a number of drawbacks associated with long-period sawteeth, resulting from sawtooth stabilisation by fast ions, were discovered. These include destabilisation of neoclassical tearing modes (NTMs) by sawtooth crashes following long-period sawteeth [6]. These have become an important issue for ITER where the fusion alpha-particles are likely to stabilise sawteeth [7]. As will be discussed in Sec. 3.1, toroidally directed ICRF waves can be used to destabilise sawteeth by current drive in the vicinity of q =1 and thereby counteract the effect of sawtooth stabilisation by fusion alpha-particles.

2.2 FUSION BY ICRF-GENERATED FAST IONS

The cross-section of deuterium-tritium (D-T) fusion reactions increases strongly with the relative velocity of the deuterium and tritium fuel ions until a maximum is reached at the energy of about 100 keV. Thus, the D-T fusion yield can be greatly enhanced by the presence of fast tritons and/or deuterons such as those injected by neutral beams and/or accelerated by ICRF waves. On JET, ICRF heating of deuterium minority ions in tritium-dominated plasmas was used to optimise the fast deuteron tail for a maximum D-T fusion reactivity. A record steady-state $Q = P_{fus}/P_{in} = 0.25$ was obtained using 6MW of ICRF alone at a plasma density of 5×10^{19} m^{-3} and a deuterium concentration of ≈10% [1]. Figure 1 shows the measured yield together with the modelled thermal and total fusion yield as given by the ICRF code PION [1, 2]. The fusion yield modelled with PION is in good agreement with the experimental fusion yield, which is an indication that the theoretical models in the field of ICRF heating are broadly adequate to describe ICRF-related effects on present-day tokamak experiments. As can be seen in Figure 1, about 90% of the fusion yield originate from fast deuterium ions. These ions have an average energy of about 100keV, which is optimal for maximising not only the fusion reactivity but also the bulk ion heating [1, 2].

2.3 MHD SPECTROSCOPY WITH ICRF-DRIVEN ALFVÈN EIGENMODES

When the ICRF-accelerated fast ions attain velocities comparable to the Alfvén speed $v_A = B/\sqrt{\mu_0 m_i n_i}$, which is a typical range of velocities of ICRF-accelerated fast ions in present-day tokamaks, they excite Alfvén Eigenmodes (AEs), typically in the range of 30-500kHz. Because the AE spectrum is uniquely determined by plasma parameters, the detection of the unstable AEs can be used to determine plasma parameters from the measured discrete Alfvén spectrum (MHD spectroscopy) [8, 9]. While providing valuable information on the plasma, the excited Alfvén waves have no detrimental effects provided the fast-ion drive, and thereby the mode amplitude, remain small. In JET plasmas, ICRF power as low as 2-4MW is sufficient to excite AEs.

Recently, the so-called AlfvÈn grand-Cascades [10] have been widely exploited in JET reversed magnetic shear discharges heated by ICRH, in order to determine times at which q_{min} passes integer values [11]. It has been found experimentally that the appearance of Alfvén grand-Cascades coincides in time with ITB triggering events observed as a sudden increase of electron temperature T_e within the q_{min} radius (Fig.2). The unique relation between Alfvén grand-Cascades, the ITB triggering events and integer q_{min} values has allowed a systematic development of ITB scenarios in JET reversed shear plasmas with different types of pre-heating scenarios.

2.4 SIMULATIONS OF FUSION-BORN ALPHA PARTICLES

The capability of ICRF waves to accelerate fast ions to energies in the MeV range has been invaluable in investigating the physics of fast ions such as fusion born alpha particles and in testing alpha diagnostics in a non-activated environment. Recently, third harmonic ion cyclotron resonance heating of ^4He beam ions has been successfully developed on JET to produce, for the first time, high-energy populations of ^4He ions to simulate 3.5MeV fusion-born alpha particles [12]. Strongest fast ^4He populations have been obtained with highest (120 keV) energy ^4He beam seed ions, as expected. Acceleration of ^4He ions to the MeV energy range was confirmed by γ-ray emission from the nuclear reaction $^9Be(\alpha,n\gamma)^{12}C$ [13] and excitation of Alfvén eigenmodes. Concomitant electron heating and sawtooth stabilisation were observed, with the electron temperature and sawtooth period increasing with the fast ion energy content.

3. CURRENT DRIVE WITH ICRF WAVES

Due to their average finite $k_{||}$, toroidally directed waves couple asymmetrically to ions and electrons in the $v_{||}$ space and can drive current. A number of current drive scenarios are possible and will be discussed in this section. Ion Cyclotron Current Drive (ICCD) and ICRF mode conversion current drive can generate localised on-axis and off-axis current and thus provide valuable alternatives for local current profile control using Electron Cyclotron Current Drive (ECCD). Fast Wave Electron Current Drive (FWCD) has typically a broader profile and is thus more suitable for general current drive in addition to Lower Hybrid Current Drive (LHCD) and Neutral Beam Current Drive (NBCD).

3.1 ION CYCLOTRON CURRENT DRIVE

The method of driving current by heating either minority ions with toroidally directed waves at a frequency equal to the ion cyclotron frequency, or majority ions at harmonics of the cyclotron frequency, was originally proposed by Fisch [14]. Because of the Doppler shift of the cyclotron resonance, $\omega = n\omega_{ci} + k_{||} v_{||}$, directed waves interact resonantly with either co-going or counter-going ions, depending on which side of the cyclotron resonance the interaction takes place and on the direction of the wave propagation. As a result, there is an effective transfer of ions either to co-passing or counter-passing orbits, and thus a driven current. Current drive, even with toroidally symmetric spectra, is possible by trapped ions due to their finite orbit widths and due to effects of non-standard orbits [15, 16].

While the net driven current is typically rather small, the local effect of ICCD on the magnetic shear can be rather strong and effects similar to ECCD control of MHD modes can be observed. This has been clearly demonstrated in JET experiments where ion cyclotron current drive has been used to modify the magnetic shear near $q = 1$ and thereby affect the sawtooth activity. The sawtooth period has been varied in ICRF-only discharges by more than one order of magnitude due to changes in the magnetic shear near $q = 1$, using hydrogen minority ($\omega \approx \omega_{cH}$) ICCD [17, 18]. More recently, experiments have been carried out on JET with directed ICRF waves tuned to the second harmonic hydrogen resonance ($\omega \approx 2\omega_{cH}$) to affect the sawtooth period and amplitude in discharges with

ICRF only and in discharges with combined ICRF and NBI [6, 19-21]. In these experiments the m = 3, n = 2 NTM seed island has been controlled by controlling the sawtooth behaviour. By adding ICCD to destabilise sawteeth, larger beta values obtained without triggering NTMs than with ICCD applied to stabilise sawteeth (Fig.3).

3.2 ELECTRON CURRENT DRIVE

ICRF waves interact resonantly with electrons via electron Landau damping and transit time magnetic pumping when $\omega = k_{||}v_{||}$, i.e. when the parallel motion of the electron guiding centre matches the parallel phase velocity of the wave. With toroidally directed waves, the power is coupled to electrons that travel either in the co-current or counter-current direction. Current drive by damping the launched fast waves on electrons (FWCD) has been observed on many tokamaks [22-25] with current drive efficiencies up to 0.5×10^{19} A/(Wm^2) and a linear dependence with the electron temperature, in good agreement with theoretical predictions (Fig.4) [22]. The driven current is centrally peaked and, consequently, FWCD is considered as one of the means to drive current in the plasma centre in ITER, thereby complementing the bootstrap current driven off-axis. Current drive with ICRF mode conversion has also been observed on TFTR [26]. Up to 130kA of current has been noninductively driven, on and off axis, and the resultant current profiles have been measured [26].

4. APPLICATIONS OF LOCALISED ICRF POWER DEPOSITION

ICRF waves provide narrow and externally controllable power depositions. In this section, representative examples from recent applications using localised ICRF power depositions with ICRF mode conversion and ion cyclotron damping are presented.

4.1 ICRF MODE CONVERSION: A TOOL FOR ELECTRON TRANSPORT STUDIES

Most narrow ICRF power deposition profiles can be obtained with ICRF mode conversion (MC). The most widely used ICRF MC scheme on the present-day tokamaks is based on mode conversion in the vicinity of the ion-ion hybrid resonance layer in a plasma with two or more main ion species with comparable concentrations, such as tritium-deuterium (D-T) plasma in a reactor. In the cold plasma limit, the ion-ion hybrid resonance layer is given by $n_{||} = 1 \ \Sigma j\omega_{pj}/(\omega^2 \ \omega_{cj}^2)$ where $n_{||}$ is the wave refractive index and ω_{pj} is the plasma frequency of particle species φ [27]. The mode-converted waves damp rapidly in the vicinity of this layer, the position of which can be controlled by changing the magnetic field, wave frequency or ion species mixture. Thus, the control of the ion species mixture is a key component of ICRF MC experiments. On JET, real time control of the ion species mixture, in particular of the ^{3}He concentration in D plasma, has been developed and used in ICRF MC experiments to control power deposition [28, 29].

Due to its relatively narrow power deposition profile, ICRF MC can provide an alternative technique to electron cyclotron heating for investigations of plasma heat transport mechanisms. On the JET tokamak, a series of experiments have been recently carried out using ICRF MC power modulation to probe electron stiffness in different confinement regimes [30, 31]. By electron stiffness we mean the capability of the plasma to oppose an increase in the electron temperature gradient by driving an increase in transport. The electron heat diffusivity and ICRF power deposition profiles have been determined self-consistently by best fitting the modulation data using full transport simulations with ASTRA [32] and an empirical critical gradient transport model.

4.2 ROLE OF ICRF POWER DEPOSITION LOCALISATION IN PLASMAS WITH INTERNAL TRANSPORT BARRIERS

In the case of ion cyclotron damping, the power absorption profile from the waves to fast ions is well-localised in the vicinity of $\omega \approx n\omega_{ci}(R)$, while the final power deposition profile to bulk plasma depends on the orbit widths of the fast ions. The available techniques to control the power deposition includes the use of directed waves to induce radial pinch of resonating ions, the use of multiple frequencies and the control of the concentration of the resonating ions to affect the fast ions energy and thereby the orbit widths.

The ICRF-induced pinch of resonating ions arises as an ion interacting with a wave receives a change in toroidal momentum [33]. For a trapped particle, this leads to the radial transport of banana tips either inwards or outwards depending on the toroidal direction of the wave. For the inward pinch with waves in the co-current direction, the fast ion orbit is eventually detrapped into co-passing orbits that reside on the low field side of the resonance $\omega \approx n\omega_{ci}$ [15]. Experimental evidence of this effect has been obtained on the JET tokamak with high-power H and ^3He minority heating [34, 35].

The ICRF-induced pinch of resonating ions can be used to control the profile of fast resonating ions and thereby to affect many ICRF-related quantities, including the power deposition profiles and the driven currents. In particular, with the ICRF resonance in the plasma centre, the profiles become significantly more peaked with the ICRF-induced pinch inwards (co-current propagating waves) than with ICRF-induced pinch outwards (counter-current propagating waves). The peaking of the power deposition profile with the inward pinch is large enough to explain the better performance obtained in JET ITB plasmas with co-current propagating ICRF waves tuned to a central H resonance as compared to counter-current phasing [36]. With 5MW of ICRF power added to 12MW of NBI heating, a higher fusion reactivity and plasma energy content have been obtained with co-current propagating waves (Fig.5). Consequently, it is the co-current propagating ICRF waves that are used routinely in JET ITB plasmas.

Another example highlighting the role of ICRF power deposition in plasmas with internal transport barriers comes from Alcator C-mod. Recently, it has been found that placing the hydrogen minority resonance at approximately the half minor radius either on the low or high field side in Alcator C-mod, a transport barrier is triggered which is also localised at about r/a = 0.5 [37]. Following the transition, the central density is observed to rise and the density profile to peak, in spite of the fact that there is no core particle source. Adding power at a second ICRF frequency to heat near the plasma axis, the density peaking has been arrested as transport increases but remains a factor of two lower than it was before the ITB formation [37].

4.3 Q-PROFILE CONTROL WITH CENTRAL ICRH

Due to their narrow power deposition, ICRF waves provide a suitable tool for profile control. In Fig.6 an example is shown from recent experiments on JET with ELMy H-mode plasmas with radiative mantle using Argon impurity injection. In these plasmas ICRF heating of hydrogen minority ions with a resonance in the plasma centre has been successfully used to increase the central electron temperature in order to keep q(0) < 1 and, thereby, to maintain sawtooth activity [38]. The applied ICRF power was low, of the order of 2-3MW, in order to prevent sawtooth stabilisation by ICRF-accelerated fast ions. With added ICRF, central Argon impurity accumulation was prevented and the duration of the quasi-steady state, high performance phase was increased from $<1\tau_E$ to the whole duration of the heating, i.e. up to $9\tau_E$.

5. EFFECTS OF ICRF WAVE ON PLASMA ROTATION

As the ICRF waves are absorbed by the plasma, not only the energy but also the momentum carried by them is transferred to the plasma. For toroidally symmetric waves the total momentum injection is virtually zero, while net momentum is injected in the case of toroidally directed waves. Although the net effect is not very large for example in comparison of momentum injection by NBI on present devices, the local effect can be important. In recent experiments on the JET tokamak, a change in the toroidal plasma rotation induced by directed ICRF waves was observed for the first time [39]. This change is well understood in terms of the influence of fast resonating ions and their transfer of momentum to the thermal plasma. Toroidal rotation with symmetric ICRF spectra with no or very little momentum input has been observed on many tokamaks [40-46], but its origin is not yet fully understood. A few observations of sheared poloidal plasma rotation with ICRF waves have also been made [47-48].

6. ICRF FOR SIMULATING ALPHA-PARTICLE HEATING IN ITER

In ITER fusion-born alpha particles heat bulk electrons without fuelling and applying net torque. In most present-day tokamaks ion heating with NBI dominates and is strongly coupled with fuelling and momentum injection. High-power ion cyclotron resonance heating with toroidally symmetric ICRF waves can provide bulk electron heating via ICRF-accelerated fast ions without applying net torque and fuelling, which is similar in its characteristics to heating provided by fusion-born alpha particles. Because of this, ICRF waves have been used to test ITER burning plasma scenarios without momentum injection.

The primary mode of ITER operation is the ELMy H-mode. No large differences between NBI and ICRF have been observed with respect to power needed to obtain H-mode [49] or confinement properties [50, 51] in this mode of operation. Work has also started to study internal transport barriers with ICRF heating only, which is important for the advanced tokamak scenario development for ITER. In recent experiments on Tore Supra an electron ITB has been triggered and maintained for 2s in a reversed magnetic shear configuration with ICRF heating only [52].

7. ICRF WAVES FOR PLASMA START-UP AND WALL CONDITIONING

In future reactor-scale superconducting fusion devices such as ITER, the presence of permanent high magnetic field prevents the use of glow discharge conditioning, which is presently the preferred method for wall conditioning. The need of controlled and reproducible plasma start-up and tritium removal, e.g. from the co-deposited carbon layers, requires alternative wall conditioning procedures. Discharge conditioning with waves in the electron and ion cyclotron range of frequencies (ECRF-DC and ICRF-DC, respectively) is fully compatible with the presence of a magnetic field. ICRF-DC has been developed in TEXTOR [53,54], TORE SUPRA [55] and HT-7 [56] using the present generation ICRF antennas without changes in hardware.

On TEXTOR, ICRF-DC wall-conditioning efficiency has been compared with that of ECRF-DC [57]. The hydrogen removal rate has been found to be about 20 times higher in ICRF-DC discharges ($\omega \approx 2\omega_{ci}$) than in ECRF-DC discharges ($\omega \approx 2\omega_{ce}$) produced by a focused microwave beam (Fig.7). The most probable reason for this is the more homogeneous plasma density profile and the generation of high-energy ions with ICRF-DC. High-energy ions in the range $E_i \approx$ 4.4-55keV have been detected in ICRF-DC discharges [54-56].

In the ITER start-up, the inductive electric field is limited to $E \approx 0.3$ V/m to prevent a quench in the superconducting coils. To perform start-up reliably at such low electric field, non-inductive pre-ionisation, target plasma production and preheating are needed. ICRF-assisted low-V_{loop} start-up has been successfully tested on TEXTOR [58]. The two pairs of the ICRF double-loop antennas without a Faraday shield, driven in π-phase, have been used for start-up assistance. The standard $2\omega_{ci}$ scenario of RF power coupling ($f = 32.5$ MHz, $P_{ICRF} \approx 200$-300 kW, $B_T = 2.24$ T) was used for the pre-ionisation and target plasma pre-heating. ICRF-assisted start-up has been achieved at the central inductive electric field $E_0 \approx 0.32$ V/m, which meets ITER requirements. Without assistance, E_0 is about 0.45 V/m. ICRF assisted start-up has been found more prompt and robust than non-assisted one and has resulted in a significantly (about 4 times) broader pressure range for current initiation, with about 22% higher current ramp-up rates.

CONCLUSIONS

Interaction of ICRF waves with the plasma has a number of key properties that make them attractive for applications beyond pure heating. In particular, ICRF waves couple power resonantly either on electrons or ions, modify the distribution functions of the resonant ions, transfer momentum to the plasma and provide narrow and externally controllable power deposition. These properties are successfully used in present-day tokamak experiments and will find applications in ITER. In particular, ICRF waves can be used to drive current, control the plasma pressure and current profile, affect plasma stability and transport, simulate fusion born alpha-particles and their effects on the plasma, and provide a diagnostics tool for plasma properties such as the evolution of q profile and transport. Furthermore, ICRF waves can be used for low-V_{loop} plasma start-up assist and wall-conditioning.

ACKNOWLEDGEMENT

This work has been performed under the European Fusion Development Agreement. The authors wish to thank Drs R. Buttery (UKAEA), F. Crisanti (ENEA Frascati), T. Hellsten (VR), L.C Ingesson (EFDA-CSU Garching), D. Moreau (CEA), F. Nguyen (CEA), E. Righi (European Commission), J. Stober (IPP Garching) and D. Van Eester (ERM) for valuable discussions.

REFERENCE

[1]. D.F.H. Start, *et al*., Phys. Rev. Lett. **80** (1998) 4681.
[2]. L.-G. Eriksson, *et al.,* Nucl. Fusion **39** (1999) 337.
[3]. D. J. Campbell, *et al*., Phys. Rev. Lett. **60** (1988) 2148.
[4]. C.K. Phillips, *et al*., Phys. Fluids **B4** (1992) 2155.
[5]. F. Porcelli, Plasma Phys. Control. Fusion **33** (1991) 1601.
[6]. O. Sauter, *et al*., Phys. Rev. Lett. **88** (2002) 105001:1.
[7]. F. Porcelli, D. Boucher and M.N. Rosenbluth, Plasma Phys. Control. Fusion 38, 2163 (1996).
[8]. T. Stix, Phys. Fluids **1** (1958) 308.
[9]. J.P. Goedbloed *et al*., Plasma Phys. Contr. Fusion **35** (1993) B277.
[10]. S.E. Sharapov, *et al*., Phys. Plasmas **9** (2002) 2027.
[11]. S.E. Sharapov, *et al*., Phys. Lett. **A289** (2001) 127.
[12]. M.J. Mantsinen, *et al*., Phys. Rev. Lett. **88** (2002) 105002:1.
[13]. V.G. Kiptily, *et al.,* Nucl. Fusion **42** (2002) 999.
[14]. N.J. Fisch, Nucl. Fusion **21** (1981) 15.
[15]. T. Hellsten, J. Carlsson, L-G Eriksson, Phys. Rev. Letters **74** (1995) 3612.
[16]. J. Carlsson, T. Hellsten, J. Hedin, Phys. Plasmas **5** (1998) 2885.
[17]. D.F.H. Start, *et al*., in Proceedings of the International Conference on Plasma Physics, Innsbruck, 1992 (European Physical Society, Geneva, 1992), Vol. **16C**, Part II, p. 897.
[18]. V.P. Bhatnagar, *et al*., Nucl. Fusion **34** (1994) 1579.
[19]. M.-L. Mayoral, *et al*., in Radio Frequency Power in Plasmas (14th Topical Conference, Oxnard, California 2001), AIP Conference Proceedings **595**, American Institute of Physics, New York (2001), p. 106.
[20]. E. Westerhof, *et al*., Nucl. Fusion **42** (2002) 1324.
[21]. M.J. Mantsinen, *et al*., Plasma Phys. Control. Fusion **44** (2002) 1521.
[22]. C.C. Petty, *et al*., Nucl. Fusion **39** (1999) 1369.
[23]. C.C. Petty, *et al*., Nucl. Fusion **35** (1995) 773.
[24]. Tore Supra Team (presented by B. Saoutic), Plasma Phys. Control. Fusion **36** (1994) B123.
[25]. R. Majeski, *et al*., Phys. Plasmas **3** (1996) 2006.
[26]. R. Majeski, *et al*., Phys. Rev. Lett. **76** (1996) 764.
[27]. T.H. Stix, Nucl. Fusion **15** (1975) 737.
[28]. E. Joffrin, *et al*., Plasma Phys. Control. Fusion (in press).

[29]. D. Van Eester, *et al*., in Radio-Frequency Power in Plasmas (Proc. 15th Topical Conference on Radio Frequency Power in Plasmas May, 2003, Moran, WY, USA), AIP, New York (in press).

[30]. P.Mantica, *et al*., 19th IAEA Fusion Energy Conference, October 2002, Lyon, France, paper EX/P1-04

[31]. P. Mantica, *et al*., 30th European Physical Society Conference on Plasma Physics and Controlled Fusion, July 2003, St. Petersburg, Russia, Europhysics Conference Abstracts (in press).

[32]. G. Pereverzev, P.N.Yushmanov, Max-Planck-IPP Report, IPP 5/98 (2002).

[33]. L. Chen, J. Vaclavik, and G. Hammett, Nucl. Fusion **28** (1988) 389.

[34]. L.-G. Eriksson, *et al*. Phys. Rev. Lett. **81** (1998) 1231.

[35]. M.J. Mantsinen, *et al*., Phys. Rev. Lett. **89** (2002) 115004:1.

[36]. M.J. Mantsinen, *et al*., Nuclear Fusion **40** (2000) 1773.

[37]. J.E. Rice, *et al*., Nucl Fusion **42** (2002) 510.

[38] M.F.F. Nave, *et al*., Proc. 28th EPS Conference on Controlled Fusion and Plasma Physics, Funchal, 2001, Europhysics Conference Abstracts Vol. 25 A (European Physical Society, Geneva, 2001) p. 961.

[39]. L.-G. Eriksson, *et al*., in Radio-Frequency Power in Plasmas (Proc. 15th Topical Conference on Radio Frequency Power in Plasmas May, 2003, Moran, WY, USA), AIP, New York (in press).

[40]. L.-G. Eriksson, *et al*., Plasma Phys. Control. Fusion **34** (1992) 863.

[41]. L.-G. Eriksson, E. Righi and K.D. Zastrow, Plasma Phys. Control. Fusion **39** (1997) 27.

[42]. J.E. Rice, *et al*., Nucl. Fusion **38** (1998) 75.

[43]. J.E. Rice, *et al*., Nucl. Fusion **39** (1999) 1175.

[44]. L.-G. Eriksson, G.T. Hoang and V. Bergeaud, Nucl. Fusion **41** (2001) 91.

[45]. G.T. Hoang, *et al*., in Radio Frequency Power in Plasmas (14th Topical Conference, Oxnard, California 2001), AIP Conference Proceedings **595**, American Institute of Physics, New York (2001), p. 138.

[46]. J.-M. Noterdaeme, *et al*., Nucl. Fusion **43** (2003) 274.

[47]. C.K. Phillips, *et al*., Nucl. Fusion **40** (2000) 461.

[48]. C.Castaldo, *et al*., 19th IAEA Fusion Energy Conference, 14- 19 October 2002, Lyon, France, paper EX-W.

[49]. E. Righi, *et al*., Report JET-P(97)28 (JET Joint Undertaking, Abingdon, 1997).

[50]. J.-M. Noterdaeme, *et al*., In Radio Frequency Power in Plasmas (13th Topical Conference, Annapolis, Maryland, 1999), AIP Conference Proceedings **485**, American Institute of Physics, New York (1999), p. 92

[51]. JET Team (prepared by F. Rimini and G. Saibene), Nucl. Fusion **42** (2002) 86.

[52]. G.T. Hoang, et al., Phys. Rev. Lett. **84** (2000) 4593.

[53]. H.G. Esser, *et al.,* Journal of Nuclear Materials **241-243** (1997) 861.

[54]. A. Lyssoivan, *et al*., in Proc. 2nd Europhysics Topical Conf. on Radio Frequency Heating and Current Drive of Fusion Devices, Brussels 1998, Vol. **22A**, p.85.

[55]. E. De la Cal and E. Gauthier, Plasma Phys. and Contr. Fusion **39** (1997) 1083.
[56]. J.K. Xie, *et al*., Journal of Nuclear Materials **290-293** (2001) 1155.
[57]. A. Lyssoivan, *et al*., in Proc. AIP 14th Topical Conf. on Radio Frequency Power in Plasmas, Oxnard 2001, Vol. **595**, p.146.
[58]. R. Koch, *et al*., in Proc. 26th EPS Conf. on Contr. Fusion and Plasma Phys., Maastricht 1999, ECA Vol. **23J** (1999), p.745.

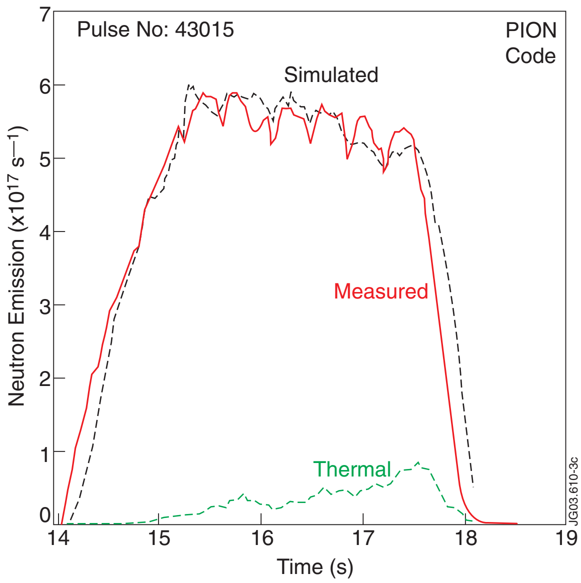

Figure 1: Measured neutron yield, together with the modelled thermal and total neutron yields as given by the ICRF code PION, for a JET plasma with a record steady-state $Q = P_{fus}/P_{in} = 0.25$ obtained using ICRF heating of deuterium minority ions in a tritium-dominated plasma [1, 2].

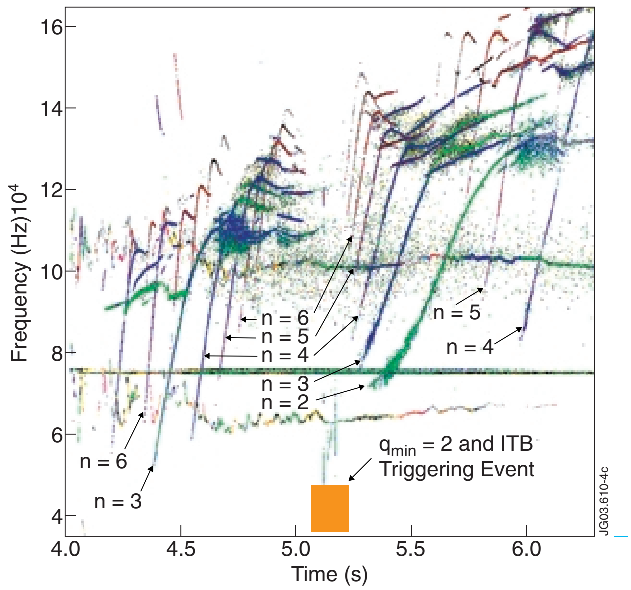

Figure 2: Magnetic fluctuation spectrogram showing the appearance of an Alfvén grand cascade consisting of many modes with different toroidal mode numbers in JET reversed shear plasma when $q_{min} = 2$ at $t \approx 5.1s$. The appearance of the Alfvén grand cascade coincides with an ITB triggering event, observed as a sudden increase of electron temperature within the q_{min} radius.

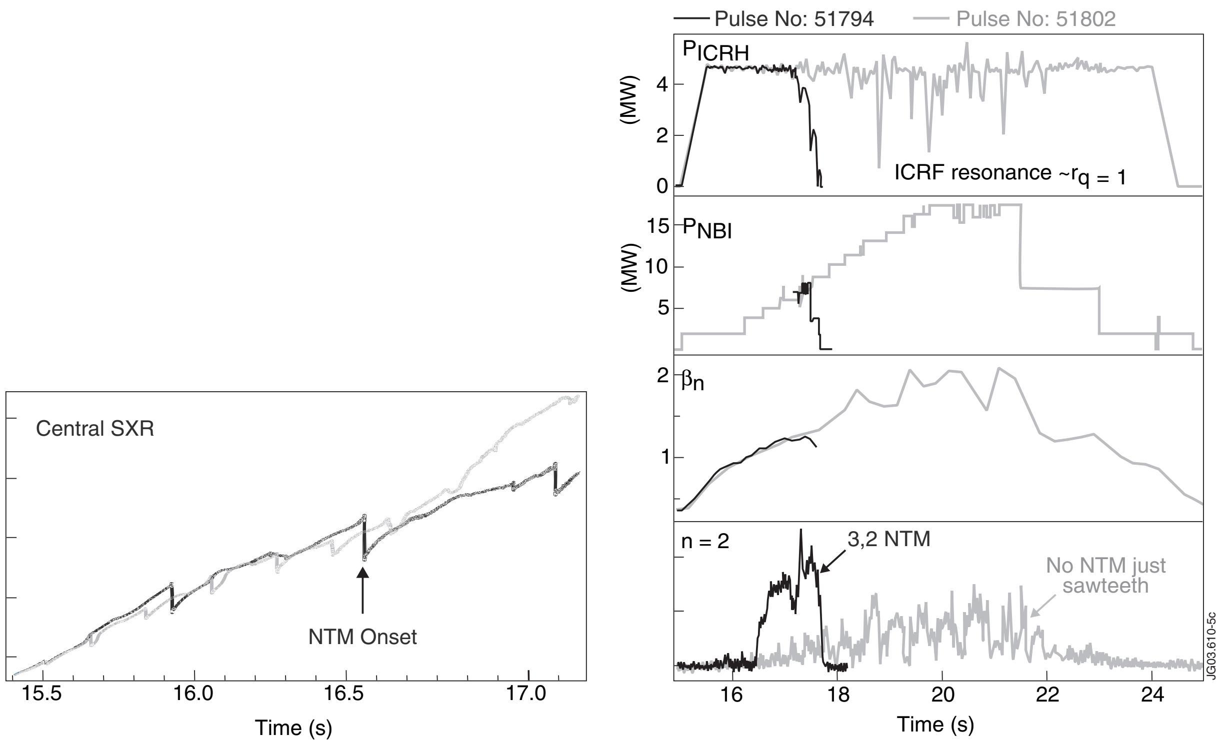

Figure 3: Comparison of two JET discharges with ICCD applied with a resonance close to q = 1 surface but with different ICRF phasings [6]. In discharge where sawteeth are destablised with ICCD, larger beta values obtained without triggering NTMs.

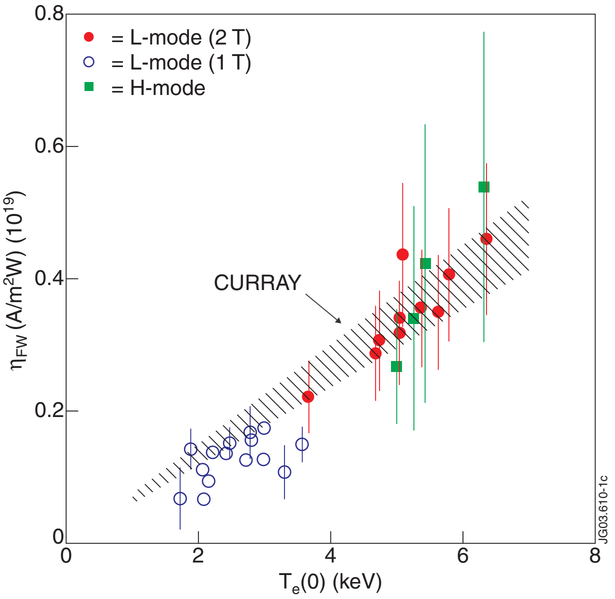

Figure 4: Comparison of the measured and modelled fast wave current drive efficiency on DIII-D [22].

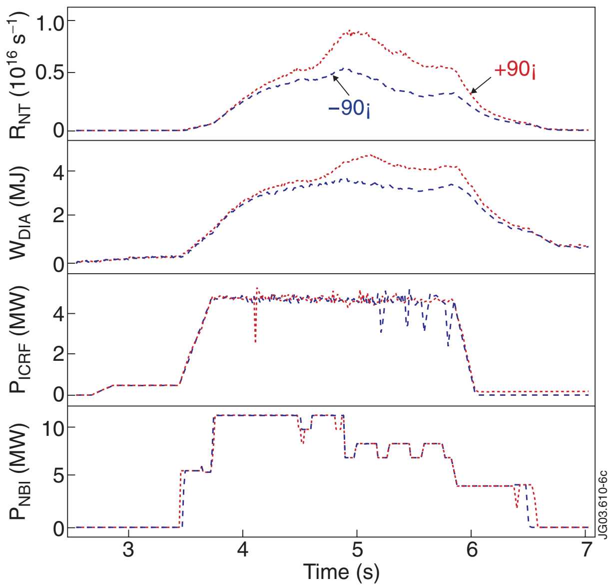

Figure 5 Comparison of two JET optimised shear plasmas with ICRH applied using +90∫ and –90∫ phasing to launch waves predominantly in the co-current and counter-current direction, respectively†[36].

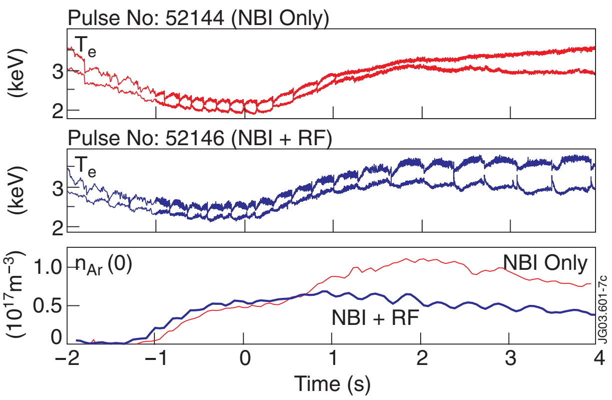

Figure 6 Comparison of two ELMy H-mode plasmas with radiative mantle using Argon impurity seeding, one with NBI heating only and the other one with combined NBI and low-power ICRF heating with a central resonance.

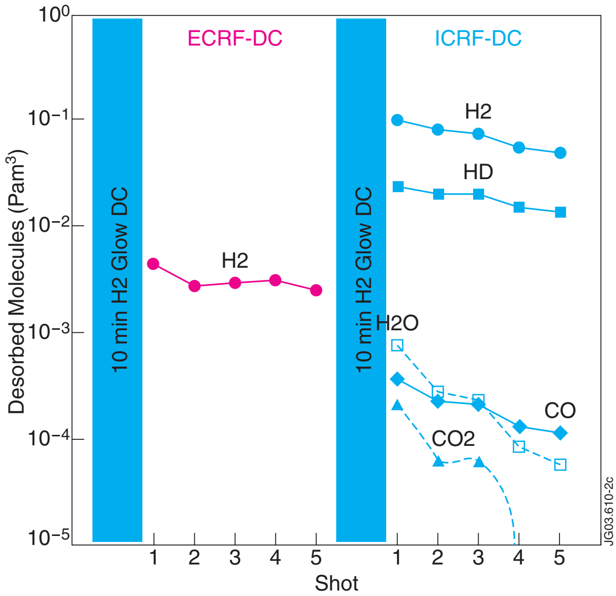

Figure 7 Comparison of H_2 desorption rates in a series of ECRF-DC and ICRF-DC discharges following H_2 glow DC on TEXTOR (B_T =2.0 T, p_{He} =2.5×10^{-2} Pa, P_{ECRF}=150 kW, P_{ICRF}=60 kW). Also, the desorption rates of HD, H_2O, CO and CO_2 are shown for ICRF-DC. No significant desorption of HD, H_2O, CO and CO_2 was observed with ECRF-DC.